

Article

Development and Assessment of a Water-Based Drilling Fluid Tackifier with Salt and High-Temperature Resistance

Yue Gao ^{1,*},[†] , Xiaobo Wang ^{2,3},[†], Yun Cheng ^{2,*}, Xuan Qi ¹ and Hao Yan ¹

¹ College of Chemical and Materials Engineering, Hainan Vocational University of Science and Technology, Haikou 571126, China; 7duan@163.com (X.Q.); yanhao0898@126.com (H.Y.)

² School of Environmental & Safty Engineering, Liaoning Petrochemical University, Fushun 113001, China; xiaobowang@163.com

³ Henan Xintai Energy Co., Ltd., Xinxiang 453000, China

* Correspondence: yueyuezcs@163.com (Y.G.); chy_ah@163.com (Y.C.)

[†] These authors contributed equally to this work.

Abstract: A high-temperature-resistant copolymer thickener (DT) was synthesized through free radical polymerization, utilizing monomers such as N-vinylformamide (NVF), divinylbenzene (DVB), and acrylamide (AM) as the primary raw materials. The polymer system's structure was characterized using FTIR and ¹H NMR, while its thermal properties were analyzed through thermogravimetric analysis. The viscosity changes of the polymers were evaluated before and after high-temperature aging at various temperatures. The results indicated that the viscosity retention rate of the thickener DT in the base slurry at 240 °C and 15% NaCl was 87.1%. Additionally, it exhibited varying anti-aging cycles between 200 °C and 240 °C. In a slurry with 25% NaCl, the viscosity retention rate reached 130% at 200 °C. High-temperature and high-pressure rheological tests demonstrated that drilling fluids containing DT exhibit consistent rheological behavior within the temperature range of 150 °C to 180 °C, which aids in stabilizing the viscosity and strength of drilling fluids at elevated temperatures.

Keywords: diethylbenzene; high-temperature resistance; thickener; anti-aging; constant rheological behavior



Academic Editors: Katarzyna Panasiuk, Sebastian Sławski and Karolina Ewelina Mazur

Received: 17 December 2024

Revised: 9 January 2025

Accepted: 12 January 2025

Published: 16 January 2025

Citation: Gao, Y.; Wang, X.; Cheng, Y.; Qi, X.; Yan, H. Development and Assessment of a Water-Based Drilling Fluid Tackifier with Salt and High-Temperature Resistance. *Crystals* **2025**, *15*, 82. <https://doi.org/10.3390/cryst15010082>

Copyright: © 2025 by the authors. Licensee MDPI, Basel, Switzerland. This article is an open access article distributed under the terms and conditions of the Creative Commons Attribution (CC BY) license (<https://creativecommons.org/licenses/by/4.0/>).

1. Introduction

As oil and gas exploration advances in regions such as Tarim, the South China Sea, and Bohai Bay, well depths have reached 8000 m. Ultra-deep and ultra-high-temperature blocks above 200 °C are poised to become significant sources of oil and gas resources in China [1–4]. Such formations impose higher requirements for the salt resistance and temperature tolerance of drilling fluid additives. Viscosity improvers are crucial agents for maintaining the rheological properties of drilling fluids [5–7]. Current technologies can adjust rheological properties within the range of 150 °C to 180 °C [8–11], but they do not yet meet the exploration requirements in ultra-deep oil and gas fields exceeding 200 °C.

This paper addresses the technical challenges of exploration and development in ultra-deep and ultra-high-temperature blocks by designing and synthesizing a salt-resistant, high-temperature-resistant, water-based drilling fluid tackifier. This approach is based on concepts such as hydrophobic association, molecular chain rigidity, and adsorption performance [12–19], providing a reference for polymer research and development in high-temperature oil and gas exploration.

This study utilized free radical polymerization technology, employing N-vinylformamide (NVF), divinylbenzene (DVB), and acrylamide (AM) as the primary monomers to synthesize

a tetrapolymer. The synthesized tackifier exhibits the following characteristics: First, the adhesive enhancers contain both hydrophilic and hydrophobic groups, effectively expanding their network structure and enhancing high-temperature resistance. Second, the basic skeleton of the adhesive enhancer consists of C–C bonds and incorporates benzene ring structures, imparting rigidity and accommodating larger side chain groups. These side chain groups inhibit the movement of the main chain in high-temperature and high-salt environments, thereby enhancing both salt and high-temperature resistance. Third, the side chains incorporate amino or sulfonic acid groups that enhance the adhesive enhancer's salt resistance and increase the polymer's solubility.

2. Experimental

2.1. Materials and Methods

Sodium carbonate, potassium persulfate, sodium hydroxide, sodium chloride, acrylamide (AM), N-vinylformamide (NVF), and divinylbenzene (DVB) are analytically pure, while calcium chloride and DSP-2 are of industrial grade. Acetone, ethanol, and deuterated chloroform were obtained from Aladdin Reagent, while DSP-2 was sourced from Shandong Deshunyuan Petroleum Science and Technology Co., Ltd. (Dongying, China).

The equipment used includes a GJS-B12K frequency conversion high-speed mixer, GRL-BX3 portable roller heating furnace, and ZNN-D6 six-speed rotary viscometer (Qingdao Bairuida Petroleum Machinery Manufacturing Co., Ltd., Qingdao, China); WQF-520 Fourier Infrared Spectrometer (Beijing Rayleigh Analytical Instrument Company, Beijing, China); Q600 TGA-DT analyzer (TA Company, Boston, MA, USA); AntonPaar Physica MCR302 rheometer (AntonPaar Company, Graz, Austria); and AVANCE III 400 nuclear magnetic resonance spectrometer (Bruker Company, Karlsruhe, Germany).

2.2. Preparation of Tackifier

DVB and an appropriate amount of deionized water were placed in a shear emulsifying device and emulsified at 2000 r/min for 15 min to obtain a white emulsion. NVF, AM, 0.3 wt% potassium persulfate, and an appropriate amount of deionized water were added to the emulsion and emulsified at 2000 r/min for 12 min. Then, NaOH was added to adjust the solution to neutrality. The emulsion was transferred to a reaction kettle and maintained at a specific temperature for 1 h under a nitrogen atmosphere. Stirring was then stopped, and the temperature was kept constant for an additional 6 h. The resulting product was extracted with acetone and ethanol 2–3 times, then dried in a vacuum oven at 60 °C for 24 h. It was subsequently crushed and screened using a 100-mesh sieve to yield a white powder, referred to as the salt-resistant and high-temperature-resistant water-based drilling fluid tackifier (tackifier DT). The reaction equation is provided below, and the synthesis process is illustrated in Figure 1.

2.3. Property Tests of Tackifier

A 2% freshwater-based slurry was prepared by adding 15% NaCl, stirring for 1 h, and then allowing it to sit at room temperature for 24 h to obtain a brine-based slurry containing 15% NaCl.

The rheological parameters were measured using a ZNN-DbB six-speed rotary viscometer. The rheological parameters were calculated using the Bingham model. The viscosity retention rate of the base slurry is calculated as shown in Formula (1).

$$\text{Viscosity retention} = \text{apparent viscosity before aging} / \text{apparent viscosity after aging} \quad (1)$$

Definitions are as follows: Apparent viscosity before aging refers to the viscosity of the test sample before rolling aging; apparent viscosity after aging refers to the viscosity of the sample after rolling aging.

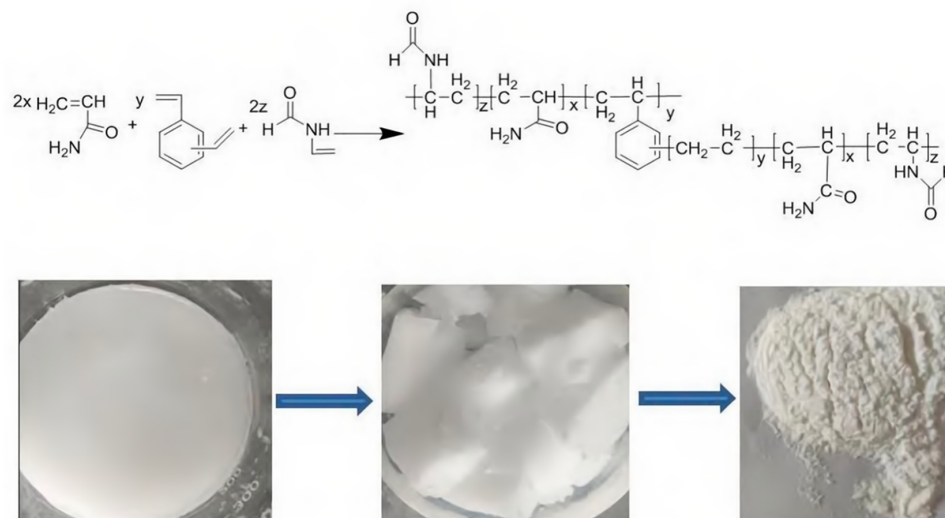


Figure 1. The process of forming white powder by shearing and drying the synthesized product.

3. Results and Discussion

3.1. The Molecular Structure of DT Was Characterized by a Fourier-Transform Infrared Spectrometer with Potassium Bromide Tablets

The synthesized DT was characterized using a Fourier-Transform Infrared Spectrometer with potassium bromide pellets.

The analysis revealed that the tensile vibration absorption peak at 3440 cm^{-1} corresponds to -NH , the peak at 2930 cm^{-1} corresponds to -CH_2 , and the resonance absorption peak at 1660 cm^{-1} corresponds to C=O . Additionally, the absorption peaks at 1510 cm^{-1} , 1450 cm^{-1} , and 1410 cm^{-1} are associated with H-C=C on the benzene rings. The tensile vibration absorption peak at 1120 cm^{-1} corresponds to C-N , while the bending vibration absorption peaks at 836 cm^{-1} , 797 cm^{-1} , and 711 cm^{-1} correspond to H-C=C on the benzene rings. In summary, the synthesized tackifier aligns with the target product, as illustrated in Figure 2.

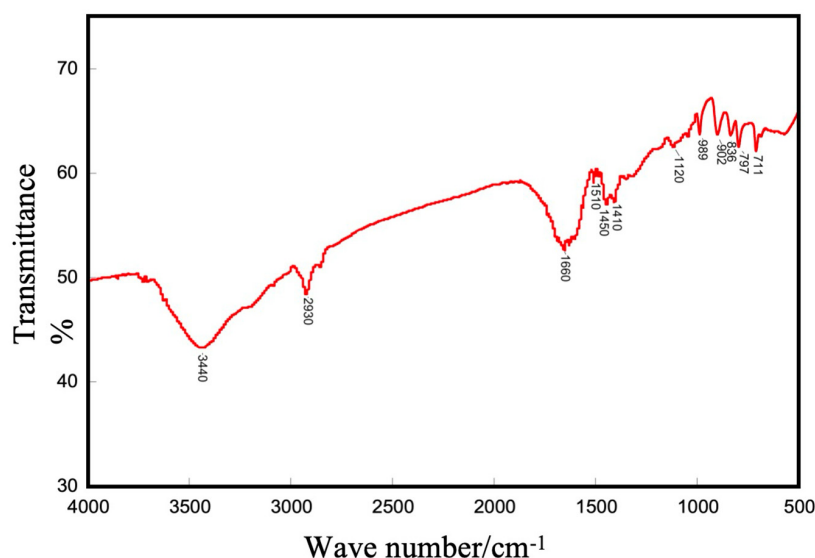


Figure 2. Infrared spectrum of tackifier DT.

3.2. $^1\text{H-NMR}$ Analysis

The $^1\text{H-NMR}$ spectrum of DT, using CDCl_3 as the solvent, shows the following: at 0.88 ppm (a), the chemical shift of hydrogen on the β carbon of NVF; at 2.61–2.68 ppm (f), the chemical shift of hydrogen on the α carbon of NVF; and at 7.34 ppm (o), the chemical shift of hydrogen directly connected to the carbonyl carbon of NVF. This confirms that NVF participates in the free radical polymerization. At 1.23 ppm (b), the chemical shift corresponds to the hydrogen on the β carbon of AM, while, at 2.02 ppm (d), it corresponds to the hydrogen on the α carbon of AM. At 1.26 ppm (c), the chemical shift corresponds to the hydrogen on the β carbon of DVB, while, at 2.22 ppm (e), it corresponds to the hydrogen on the α carbon of DVB. The shifts at 6.71 ppm (i), 7.30 ppm (j), and 7.32 ppm (k) correspond to the hydrogen on the benzene rings, confirming that DVB participated in the reaction [9]. The shifts at 5.67–5.79 ppm (g) and 5.17–5.36 ppm (h) correspond to the active hydrogens of AM and NVF, respectively. In conclusion, these results are consistent with polymer DT, as shown in Figure 3.

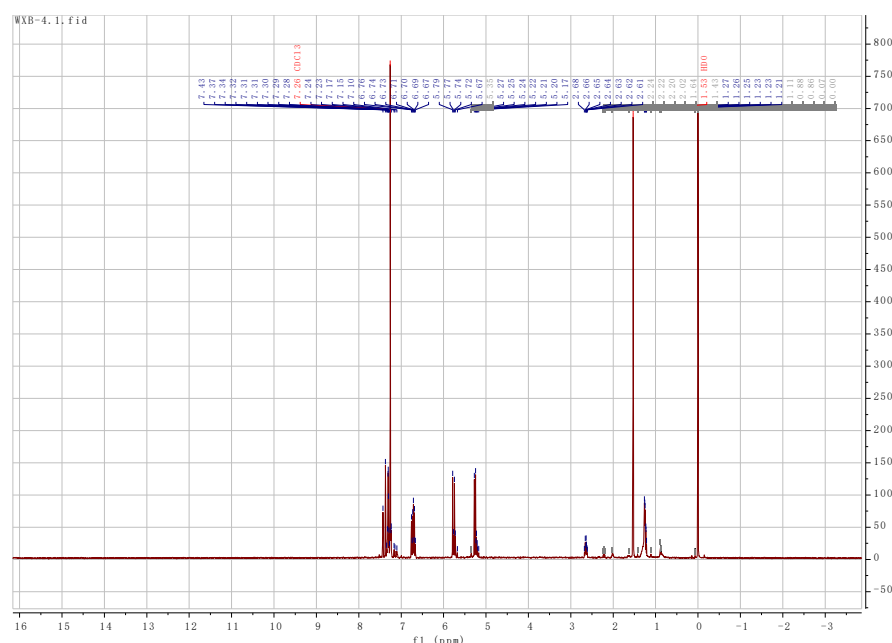


Figure 3. $^1\text{H-NMR}$ diagram of the tackifier.

3.3. Thermal Weightlessness Performance Analysis

The thermal resistance of DT was evaluated using a TGA-Q500 thermogravimetric analyzer. The weight loss of tackifier DT occurs in four stages. In the first stage, DT experiences a weight loss of 6.64% at approximately 100 °C, primarily due to the evaporation of a small amount of free water in the product. In the second stage, the mass loss of DT is 1.16% between 100 °C and 229 °C, likely resulting from the loss of bound water. In the third stage, the mass loss reaches 15.67% between 229 °C and 354 °C, primarily due to the thermal decomposition of the amide groups in the product. In the fourth stage, the mass loss of DT is 51.15% between 354 °C and 480 °C, primarily attributed to the thermal decomposition of the main chain. In summary, tackifier DT demonstrates good thermal stability, as illustrated in Figure 4.

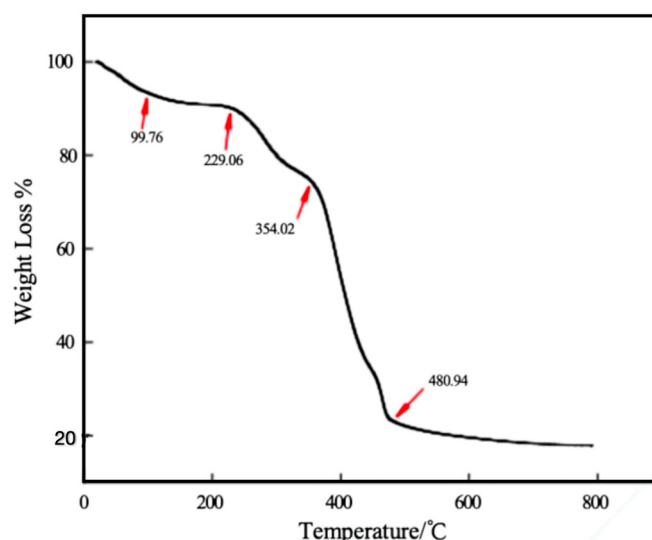


Figure 4. Thermogravimetric analysis of the tackifier.

3.4. Thermal Stability Test of Tackifier DT

A 400 mL sample of the saline-based slurry was taken, and 3% synthetic tackifier was added while stirring at 3000–6000 r/min. Note that 2%, 3%, and 4% tackifier were added to the drilling fluid, resulting in apparent viscosities of 12.5 mPa·S, 28 mPa·S, and 36 mPa·S after 16 h of high-temperature aging. The dosage of the tackifier should be determined based on oilfield operational regulations and actual conditions. After aging at 200–240 °C for 16 h, the viscosity was retested using a six-speed rotary viscometer, with the results presented in Table 1.

Table 1. Changes in viscosity of tackifier DT at 200–240 °C.

Sample	Age Condition	AV mPa·S	PV mPa·S	YP Pa	YP/PV Pa/mPa·S	Viscosity Retention Rate (%)
saline water Base slurry	Before aging	3.5	3	0.51	0.17	-
	200 °C	3	3	0	0	85.7
Saline-based slurry +3%DT	Before aging	15.5	11	4.10	0.37	-
	200 °C	28	26	2.04	0.08	180.7
	210 °C	21	14	7.15	0.51	135.5
	220 °C	29	26	3.07	0.12	187.1
	230 °C	27	22	5.11	0.23	174.2
	240 °C	13.5	11	2.56	0.23	87.1

Note: The saline-based slurry is freshly prepared before each aging. A dash (“-”) indicates that the item is not applicable (the same applies to the following experiments).

A comparison of the data in Table 1 reveals a significant increase in viscosity for both the brine-based slurry and the brine-based slurry after the addition of tackifier DT.

This indicates the excellent performance of the tackifier in enhancing viscosity. Experimental observations at high temperatures (200 °C to 240 °C) for 16 h showed that the viscosity retention rate of the drilling fluid ranged from 87.1% to 187.1%, demonstrating remarkable stability. These data clearly demonstrate the tackifier’s excellent characteristics regarding salt and high-temperature resistance.

3.5. Test of the Temperature-Resistant Period

To better evaluate the tackifier’s temperature resistance and durability, we investigated its temperature resistance period (defined as one cycle of 16 h), using the same preparation

method as previously described. After aging at 200–240 °C for n cycles (where $n = 1–4$), the viscosity was retested using a six-speed rotary viscometer. The results are presented in Figure 5 and Tables 2–4.

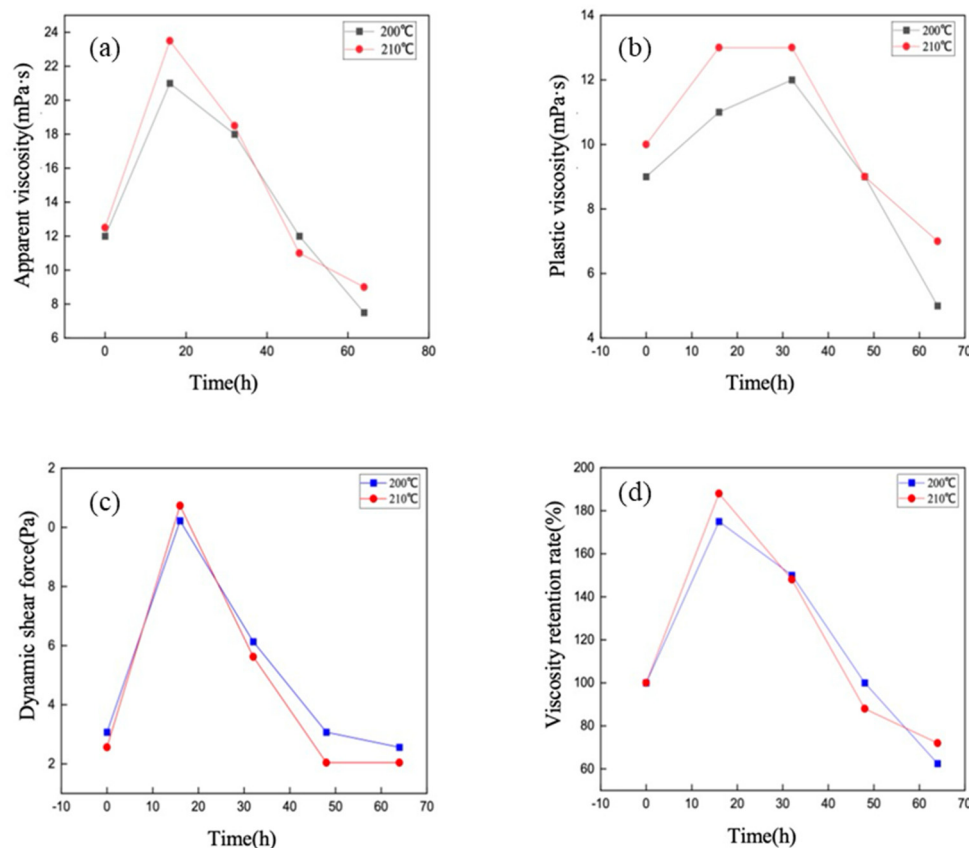


Figure 5. Effects of temperature and aging time on (a) apparent viscosity, (b) plastic viscosity, (c) dynamic shear force, and (d) changes in the viscosity retention rate.

Table 2. Effect of aging time on the viscosity enhancement performance at 220 °C.

Age Condition	Age Cycle	AV mPa·S	PV mPa·S	YP/Pa	YP/PV Pa/mPa·S	Viscosity Retention Rate (%)
room temperature	0	13	10	3.1	0.31	-
220 °C	1	18.5	10	8.7	0.87	142.3
	2	13	9	4.6	0.51	100.0
	3	9.5	6	3.6	0.60	73.1

Table 3. Effect of aging time on the viscosity enhancement performance at 230 °C.

Age Condition	Age Cycle	AV mPa·S	PV mPa·S	YP/Pa	YP/PV Pa/mPa·S	Viscosity Retention Rate (%)
room temperature	0	11.5	8	3.6	0.45	-
230 °C	1	21	11	10.2	0.93	182.6
	2	9	6	3.1	0.51	78.3

The data presented in the chart indicate that, under extreme high-temperature aging conditions, particularly during four cycles (totaling 64 h) at 200 °C and 210 °C, the tackifier’s viscosity retention rate remains above 62.5%. This clearly demonstrates the

tackifier's excellent anti-aging characteristics in high-temperature environments. However, in the more extreme range of 220–240 °C, although the tackifier did not withstand four aging cycles and the viscosity retention rate gradually decreased, it remained above 73.1% during the effective period. Notably, the bubbles generated during high-speed stirring can be eliminated after standing for some time. This may be attributed to the possibility that the tackifier's chains break during high-temperature aging (220–240 °C), leading to the formation of amphiphilic substances. Overall, these observations indicate that the tackifier exhibits excellent salt resistance, high-temperature resistance, and aging resistance, providing strong support for its broad application potential in drilling fluids.

Table 4. Effect of aging time on the viscosity enhancement performance at 240 °C.

Age Condition	Age Cycle	AV/mPa·S	PV/mPa·S	YP/Pa	YP/PV/Pa/mPa·S	Viscosity Retention Rate (%)
room temperature 240 °C	0	11.5	10	1.5	0.15	-
	1	10.5	8	2.6	0.32	91.3

Note: The absence of the second, third, or fourth aging cycle at 220–240 °C is due to the large number of bubbles generated after high-temperature aging cooling and stirring with a high-frequency high-speed mixer, which cannot measure its viscosity.

3.6. Performance Test in High-Temperature Sodium Salt

A 400 mL sample of the freshwater-based slurry was taken, and 3% synthetic tackifier was added while stirring at 3000–6000 r/min for 20 min. The rheological parameters were then measured using a six-speed rotary viscometer. Different amounts of NaCl (5%, 15%, and 25%) were added to the freshwater-based slurry, which was then aged at 200 °C for 16 h to investigate the differences in viscosity changes. See Table 5 for the data.

Table 5. Viscosity changes of different contents of NaCl added to 200 °C freshwater-based slurry.

Sample	Age Condition	AV mPa·S	PV mPa·S	YP Pa	YP/PV Pa/mPa·S	Viscosity Retention Rate (%)
Freshwater-based pulp +3%DT	0%NaCl					
	Before aging	7	6	1.02	0.17	-
	After aging at 200 °C	30	20	10.2	0.51	428
	5%NaCl					
	Before aging	8.5	6	2.56	0.43	-
	After aging at 200 °C	23	16	7.15	0.45	270.6
	15%NaCl					
	Before aging	12	9	3.07	0.34	-
	After aging at 200 °C	21	11	10.22	0.93	175
	25%NaCl					
	Before aging	10	9	1.02	0.11	-
	After aging at 200 °C	13	10	3.07	0.31	130

As the NaCl content increases, Table 5 shows that the initial viscosity of the base slurry gradually rises. However, after aging at 200 °C for 16 h, the viscosity decreases as the NaCl content increases. The increase in initial viscosity may be attributed to the tackifier's salt-sensitive nature; as the salt content rises, the viscosity also increases within a certain range. Another possibility is the aggregation of hydrophobic groups, which contributes to the increase in viscosity. However, high-temperature aging decreases the pH value, further affecting the hydration groups and diminishing the viscosity-enhancing effect of

the tackifier. In this process, it can be observed that a higher salt content correlates with a more significant decrease in viscosity.

3.7. Rheological Experiment at High Temperatures and High Pressures

The high-pressure high-temperature (HPHT) rheological characteristics of the fluid containing the tackifier are presented in Figure 6. Figure 6 indicate that the Bingham plastic model is suitable for the HPHT rheological curve of the fluid containing the tackifier.

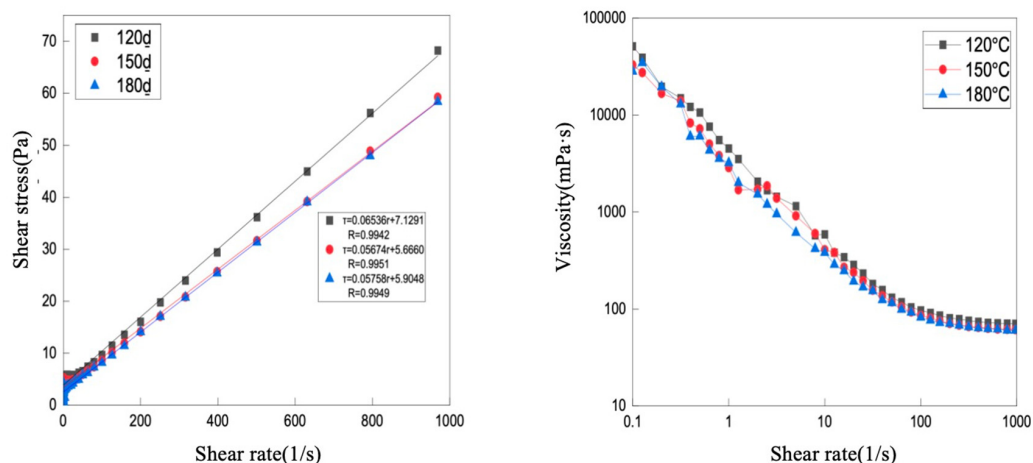


Figure 6. Rheological properties and shear thinning properties of HPHT with a viscosity-increasing agent.

Figure 6 shows that the rheological parameters of the fluid treated with DT are favorable at temperatures of 120 °C, 150 °C, and 180 °C, indicating that DT exhibits good viscosity-increasing performance under HPHT conditions. The rheological parameters of the fluid containing the tackifier respond to temperature increases. In the case of fluid containing DT at temperatures between 150 °C and 180 °C, viscosity and yield stress tend to remain stable with the increasing temperature. This stability may be related to the formation of hydrophobic association microstructures with phenyl groups in the side chains, accompanied by changes in the hydrodynamic volume of polymer molecules in solution and a transformation from loose helices to network aggregates [20]. Additionally, phase separation is prevented by the hydrophilic main chain, which stabilizes the associated phase at the microscopic level. Microstructures play a minor role in crosslinking between polymer chains, which helps maintain or increase the viscosity.

3.8. Mechanism Analysis

At room temperature, the viscosity of the polymer solution is low. However, when the temperature reaches a certain critical association temperature [21], the viscosity of the system increases rapidly. This increase may be due to the presence of both hydrophilic amide groups and hydrophobic phenyl groups in the side chains of the copolymer molecules. Above the critical association temperature, as the temperature increases, the association of hydrophobic groups in the copolymer side chains significantly enhances, leading to an increase in the mechanical volume of the copolymer molecules and, consequently, the viscosity of the solution. However, when the temperature rises beyond a certain point, the copolymer molecules may break or precipitate, resulting in a decrease in solution viscosity.

Additionally, the presence of numerous hydrophobic monomers may cause an increase in viscosity when the temperature rises to a point where hydrophobic associations significantly outweigh molecular electrostatic repulsion. The initial viscosity of the polymer solution increases slightly with the rising salt content. This is due to the natural coexistence of the polymer and salt, where the presence of salt slightly opens the polymer molecular

chains, leading to increased viscosity and salt sensitivity. Furthermore, the enhanced tackifying behavior in the presence of salt may result from the combination of strong hydrogen bonds between amino groups, a hydrophobic association network structure, and strong interactions between the tackifier and bentonite lamellae. The hydrophobic polymer achieves thixotropy in drilling fluid colloids through electrostatic adsorption–desorption with hydrated clay particles. This process avoids issues related to the simple long-chain structures of traditional treatment agents, which are prone to chain breakage and crosslinking, leading to the deterioration of the drilling fluid's rheological properties.

4. Conclusions

Tackifier DT was synthesized via free radical polymerization of DVB, AM, and NVF. The polymer's formation from these three monomers was confirmed through FTIR, ¹H-NMR, and thermogravimetric analysis.

Tests on the aging resistance, salt resistance, and temperature resistance of polymer DT concluded that it exhibits excellent aging and salt resistance at 15% NaCl and 200 °C. The viscosity retention rate remains 87.1% at 240 °C, demonstrating excellent high-temperature resistance. This study examined the effect of different NaCl concentrations on the apparent viscosity of the polymer solution, concluding that polymer DT exhibits excellent salt resistance.

High-temperature and high-pressure rheological tests indicate that DT-containing drilling fluids exhibit consistent changes in viscosity and strength within the temperature range of 150 °C to 180 °C, which stabilizes these properties at elevated temperatures. Shear tests indicate that DT exhibits a shear-thinning effect, likely related to the formation of hydrophobic association microstructures with phenyl groups in the side chains, along with changes in the hydrodynamic volume of polymer molecules in solution and a loosening of the screw structure. The transition from a rotational to a network aggregate structure leads to either an increase in viscosity or a constant viscosity.

In conclusion, tackifier DT demonstrates excellent salt resistance, high-temperature resistance, and even ultra-high-temperature resistance, making it suitable for meeting the technical requirements of drilling fluids in high-temperature and ultra-high-temperature environments. Furthermore, the preparation process and parameters for this polymer are straightforward and amenable to industrialization.

Author Contributions: Conceptualization, Y.G.; Methodology, Y.C. and H.Y.; Formal analysis, X.Q.; Investigation, X.W. All authors have read and agreed to the published version of the manuscript.

Funding: The study was supported by the university-level team research project of Hainan Vocational University of Science and Technology in 2024: "Research on Polyionic Liquid Materials and Their Catalytic Properties(HKKY2024-TD-17)"; Hainan Vocational University of Science and Technology university-level Teaching Reform Project 2025: "Research on Ideological and Political Teaching Model of 'Chemical Engineering Principles' Based on Goal and Problem Orientation (HIKJG2024-012); Research on Teaching Methods of Mechanical Manufacturing Courses under Informationization Conditions" (HKJG2024-35).

Data Availability Statement: Data are contained within the article.

Conflicts of Interest: Author Xiaobo Wang was employed by the company Henan Xintai Energy. The remaining authors declare that the research was conducted in the absence of any commercial or financial relationships that could be construed as a potential conflict of interest.

References

1. Sun, J.; Yang, J.; Bai, Y.; Lyu, K.; Liu, F. Research progress and development of deep and ultra-deep drilling fluid technology. *Pet. Explor. Dev.* **2024**, *51*, 1022–1034. [[CrossRef](#)]
2. Bai, Y.; Zhu, Y.; Sun, J.; Shang, X.; Wang, J. High stability polymer gel for lost circulation control when drilling in fractured oil and gas formations. *Geoenergy Sci. Eng.* **2023**, *225*, 211722. [[CrossRef](#)]
3. Cao, T.; Gao, Y.; Xia, W.; Qi, X. Preparation of Bi@ Ho³⁺: TiO₂/Composite Fiber Photocatalytic Materials and Hydrogen Production via Visible Light Decomposition of Water. *Catalysts* **2024**, *14*, 588. [[CrossRef](#)]
4. Medhi, S.; Chowdhury, S.; Dehury, R.; Khaklari, G.H.; Puzari, S.; Bharadwaj, J.; Talukdar, P.; Sangwai, J.S. Comprehensive review on the recent advancements in nanoparticle-based drilling fluids: Properties, performance, and perspectives. *Energy Fuels* **2024**, *38*, 13455–13513. [[CrossRef](#)]
5. Yang, H.; Pan, S.; Jiang, H.; Zhang, J.; Li, H.; Xing, L.; Zhang, Y.; Sarsenbekuly, B.; Kang, W.; Zhang, X.; et al. Study of a high salt tolerant amphiphilic polymer and its salt thickening mechanism. *J. Mol. Liq.* **2024**, *400*, 124552. [[CrossRef](#)]
6. Lalji, S.M.; Ali, S.I.; Khan, M.A. Study of rheological characteristics of a water-based drilling fluid in presence of biopolymers, synthetic polymer, and modified natural polymer. *Pet. Chem.* **2023**, *63*, 906–916. [[CrossRef](#)]
7. Dong, X.; Sun, J.; Huang, X.; Li, J.; Lv, K.; Zhang, P. Synthesis of a low-molecular-weight filtrate reducer and its mechanism for improving high temperature resistance of water-based drilling fluid gel system. *Gels* **2022**, *8*, 619. [[CrossRef](#)] [[PubMed](#)]
8. Yang, S.; Wang, H.; Wang, Y. Temperature-Sensitive Materials for Oil and Gas Drilling Applications. *Molecules* **2024**, *29*, 1471. [[CrossRef](#)] [[PubMed](#)]
9. Li, J.; Ji, Y.X.; Ni, X.X.; Lv, K.H.; Huang, X.B.; Sun, J.S. A micro-crosslinked amphoteric hydrophobic association copolymer as high temperature-and salt-resistance fluid loss reducer for water-based drilling fluids. *Pet. Sci.* **2024**, *21*, 1980–1991. [[CrossRef](#)]
10. Yang, Z.; Zhang, Y.; Zhang, X.; Wang, T.; Wang, Q. Research Progress of High Temperature Shape Memory Polymers. *J. Funct. Polym.* **2022**, *35*, 314–327.
11. Wang, Z.; Sun, J.; Zhang, K.; Lv, K.; Huang, X.; Wang, J.; Wang, R.; Meng, X. A temperature-sensitive polymeric rheology modifier used in water-based drilling fluid for deepwater drilling. *Gels* **2022**, *8*, 338. [[CrossRef](#)] [[PubMed](#)]
12. Shi, S.; Sun, J.; Lv, K.; Liu, J.; Bai, Y.; Wang, J.; Huang, X.; Jin, J.; Li, J. Fracturing fluid polymer thickener with superior temperature, salt and shear resistance properties from the synergistic effect of double-tail hydrophobic monomer and nonionic polymerizable surfactant. *Molecules* **2023**, *28*, 5104. [[CrossRef](#)] [[PubMed](#)]
13. Misbah, B.; Sedaghat, A.; Balhasan, S.; Elgaddafi, R.; Malayer, M.A.; Malhas, R.N.; Omar, M.; Benomran, M. Enhancing thermal stability and filtration control for water-based drilling fluid using viscosifier polymers and potassium chloride additives. *Geoenergy Sci. Eng.* **2023**, *230*, 212235. [[CrossRef](#)]
14. Liu, P.; Yang, X.; Chen, W.; Hao, Y. Preparation of the modified chitosan flocculant introduced acryloyloxyethyl trimethyl ammonium chloride and 2-acrylamido-2-methyl propane sulfonic acid for the treatment of papermaking wastewater. *Colloids Surf. A Physicochem. Eng. Asp.* **2024**, *682*, 132934. [[CrossRef](#)]
15. Tang, J. Heat-Induced Structural Modifications of Plant Proteins: Implications for Peptide Pattern and Bioactivity After Infant Digestion. Ph.D. Thesis, Wageningen University and Research, Wageningen, The Netherlands, 2024.
16. Gao, Y.; Meng, Q.-B.; Wang, B.-X.; Zhang, Y.; Mao, H.; Fang, D.-W.; Song, X.-M. Polyacrylonitrile Derived Robust and Flexible Poly (ionic liquid) s Nanofiber Membrane as Catalyst Supporter. *Catalysts* **2022**, *12*, 266. [[CrossRef](#)]
17. Mao, J.; Xue, J.; Zhang, H.; Yang, X.; Lin, C.; Wang, Q.; Li, C.; Liao, Z. Investigation of a hydrophobically associating polymer's temperature and salt resistance for fracturing fluid thickener. *Colloid Polym. Sci.* **2022**, *300*, 569–582. [[CrossRef](#)]
18. Fan, M.; Lai, X.; Li, J.; Wang, T.; Wang, L.; Gao, J.; Wen, X.; Liu, G.; Liu, Y. Rheological properties and ultra-high salt resistance of novel hydrophobically associating copolymers for fracturing fluids. *Polym. Bull.* **2023**, *80*, 8725–8743. [[CrossRef](#)]
19. Deng, H.; Tao, H.; Ai, J.; Chen, J.; Xie, B.; Djouonkep, L.D.W. Preparation and evaluation of an ultra-high temperature resistant zwitterionic polymer viscosity reducer. *J. Polym. Res.* **2024**, *31*, 71. [[CrossRef](#)]
20. Liu, X.; Hou, Y.; Zhang, Y.; Zhang, W. Thermoresponsive Polymers of Poly(2-(N-alkylacrylamide)ethyl acetate)s. *Polymers* **2020**, *12*, 2464. [[CrossRef](#)] [[PubMed](#)]
21. Song, X.; Li, G.; Huang, Z.; Shi, Y.; Wang, G.; Song, G.; Xu, F. Review of high-temperature geothermal drilling and exploitation technologies. *Gondwana Res.* **2023**, *122*, 315–330. [[CrossRef](#)]

Disclaimer/Publisher's Note: The statements, opinions and data contained in all publications are solely those of the individual author(s) and contributor(s) and not of MDPI and/or the editor(s). MDPI and/or the editor(s) disclaim responsibility for any injury to people or property resulting from any ideas, methods, instructions or products referred to in the content.